

Energetics and Luminosity Function of Gamma-ray Bursts

Pawan Kumar

JILA, Boulder, CO 80303, and IAS, Princeton, NJ 08540

Tsvi Piran

Racah Institute, The Hebrew University, Jerusalem 91904, Israel

Received _____; accepted _____

arXiv:astro-ph/9909014v1 1 Sep 1999

ABSTRACT

Gamma-ray bursts are believed to be some catastrophic event in which material is ejected at a relativistic velocity, and internal collisions within this ejecta produce the observed γ -ray flash. The angular size of a causally connected region within a relativistic flow is of the order the angular width of the relativistic beaming, γ^{-1} . Thus, different observers along different lines of sights could see drastically different fluxes from the same burst. Specifically, we propose that the most energetic bursts correspond to exceptionally bright spots along the line of sight on colliding shells, and do not represent much larger energy release in the explosion. We calculate the distribution function of the observed fluence for random angular-fluctuation of ejecta. We find that the width of the distribution function for the observed fluence is about two orders of magnitude if the number of shells ejected along different lines of sight is ten or less. The distribution function becomes narrower if number of shells along typical lines of sight increases. The analysis of the γ -ray fluence and afterglow emissions for GRBs with known redshifts provides support for our model i.e. the large width of GRB luminosity function is not due to a large spread in the energy release but instead is due to large angular fluctuations in ejected material. We outline several observational tests of this model. In particular, we predict little correlation between the γ -ray fluence and the afterglow emission as in fact is observed. We predict that the early (minutes to hours) afterglow would depict large temporal fluctuations whose amplitude decreases with time. Finally we predict that there should be many weak bursts with about average afterglow luminosity in this scenario.

Subject headings: gamma rays: bursts – relativistic shock

1. Introduction

The improvement in the determination of angular position of GRBs by the Dutch–Italian satellite, BeppoSAX, has led to measurement of distances to eight GRBs and has lent support for the relativistic shock model (cf. Costa et al. 1997, van Paradijs et al. 1997, Bond 1997, Frail et al. 1997). Unlike previous expectations these observations revealed that the GRB luminosity function is very broad; the width of the fluence distribution is about two orders of magnitude in energy. Assuming isotropic emission one finds that the energy of the most energetic bursts is larger than 10^{54} ergs. The recently observed evidence for beaming with an opening angle of a few degrees reduces the energy estimate by a factor of a hundred (Kulkarni et al., 1999; Sari, Piran & Halpren, 1999; Harrison et al., 1999). However, when taking into consideration the relatively low efficiency of conversion of kinetic energy to γ -rays, one finds that the total kinetic energy required is, after all, of order 10^{54} erg even after the beaming correction (Kumar, 1999). This energy is too large to be released by a compact solar mass object. According to the internal-external shock model comparable amount of energy should be released during the GRB phase and the afterglow. However, quite generally, only a fraction of the energy emitted as γ -rays is seen in the afterglow (mostly as X-rays). Moreover, there appears to be little correlation between the γ -ray fluence and the afterglow flux.

All the above mentioned phenomena could be unrelated. However, within the framework of relativistic internal shocks model (Narayan, Paczynski & Piran, 1992, Paczynski & Xu 1994, Rees & Mészáros 1994, Sari & Piran 1997) we suggest a possible connection: these properties could all be manifestations of large angular inhomogeneity of the relativistic ejecta. The size of a causally connected region of a shell of radius R moving with Lorentz factor γ is $\sim R/\gamma$. Because of relativistic beaming this is also the size of the region visible to a distant observer. During the GRB the angular size of these regions (< 0.01 rad) is significantly smaller than the inferred angular width of the ejecta, $\delta\theta \sim$ a few degrees. There are therefore $(\gamma\delta\theta)^2$ causally disconnected regions within this cone. Thus the observed γ -ray luminosity seen by different observers from the same burst could fluctuate strongly due to small scale inhomogeneities in the emitting regions. Unless careful, one would over-estimate the energy release in γ -rays in cases in which a hot spot has been observed¹. At a later time when the Lorentz factor of the ejecta has become smaller and the size of causally connected regions is larger the dispersion of the afterglow luminosity seen along different lines of sight should be smaller as well. The emission at this stage yields a better estimate of the overall total energy involved.

¹Note that as BeppoSAX can detect only rather strong bursts the BeppoSAX sample might be biased towards cases in which such a hot spot has been seen.

We explore, here, the implications of this model. The model is presented in the next section, followed by calculation of the distribution of fluence. The observational aspects are discussed in section 3, and the main results and some predictions of the model are summarized in section 4.

2. The Physical Model and Numerical simulation

The calculations described in this section are numerical, but in §2.2 we analyze a simple model analytically to gain some insight into the numerical results.

We consider successive, random, ejection of blobs of angular size γ^{-1} into a cone with an opening angle $\delta\theta = 10^\circ$. To estimate the expected fluence distribution we have carried out Monte Carlo simulations of the observed emission from randomly ejected shells - corresponding to the random conditions expected in different causally disconnected regions. In each case we keep the overall energy ejected into a given cone of opening angle 10° approximately the same - 10^{52} ergs. Changing the total energy in bursts causes a linear translation of the fluence distribution function. The Lorentz factor of each shell is assumed to be a random number uniformly distributed between γ_{min} and γ_{max} ; we take $\gamma_{min} = 5$ & $\gamma_{max} = 400$. The energy distribution of blobs is taken to be either log-normal with mean of $10^{52}/N_b$ erg and width (FWHM) in $\log_{10}(\text{energy})$ of 1, or a delta function distribution; N_b is the number of blobs ejected in the explosion. The number of blobs ejected along a line of sight is also taken to be a random number uniformly distributed between N_{min} and N_{max} . We have considered two different values for the average number of shells ejected: $(N_{min} + N_{max})/2$ equal to 5 and 40. The shells are ejected randomly over some time interval corresponding to the total duration of 30 s.

The calculation and the results described here apply to the case where shells have little or no angular fluctuation, and the radiation received by different observers located within 10° cone is a smooth function. The distribution function for fluence in this case is significantly narrower compared to when shells have large angular fluctuations (see §2.1).

We consider all possible shell collisions along a line of sight, and for each collision we follow the forward and reverse shocks propagating within the colliding shells. The thermodynamic properties of the shocked gas are calculated by solving the continuity of energy, momentum, and baryon number flux (see e.g. Piran 1999). Shell collisions continue until mergers arrange the shell velocities as a monotonically increasing function of their distance from the center of explosion. We assume equipartition of energy between electrons, protons and magnetic field (the energy fraction in magnetic field $\epsilon_B = 0.3$, and in the electrons $\epsilon_e = 0.3$). The distribution of electron number density is taken to be a power-law function of energy, $n_e(E) \propto E^{-p}$, with $p = 2.5$.

We calculate synchrotron emission from relativistic electrons and include the effect of electron cooling and inverse-synchrotron absorption on the power spectrum (e.g. Sari, Piran & Narayan, 1998). The synchrotron photons undergo inverse Compton scattering to produce the emergent spectrum (we calculate multiple Compton scatterings when the Compton y -parameter is greater than 1). As photons emitted by one shell might undergo elastic collisions in other shells we follow the trajectory of photons produced in shell collisions, along with the trajectory of different shells, to determine the energy and momentum deposited by photons in different shells and the resulting change to the bulk kinetic energy of shells (Kumar, 1999).

The computed emergent power spectrum is integrated between 10–10³ keV, in the observer frame, to determine fluence along different lines of sight. From the ‘observed’ fluence we calculate the isotropic radiative energy in γ -rays (it should be emphasized, however, that the radiation is highly anisotropic when shells are not uniform). The total energy in explosion is obtained by adding the energy of all the blobs in a cone of 10° opening angle, which as stated previously is taken to be 10⁵² erg.

2.1. Fluence distribution and Burst Energetics

Figure 1 shows the isotropic γ -ray fluence distribution resulting from the calculation described above where the total energy in the explosion is 10⁵² erg. The full width at half maximum (FWHM) of $\log_{10}(\text{fluence})$ distribution function is about 2.0, i.e. two orders of magnitude in the linear energy scale, when the mean number of shells along the line of sight is 5 and the FWHM of the energy distribution of individual blobs is 1.0 (on \log_{10} scale). Part of the width of the fluence distribution results from the energy distribution of blobs, and rest from the distribution of their Lorentz factor. The FWHM of the fluence distribution function is 1.2, i.e. a factor of 15 on linear scale, when the energy of blobs follows a delta-function distribution. Clearly in this case fluence distribution is a result of the fluctuation in the radiative efficiency of internal shocks.

The width of the fluence distribution function decreases with increasing number of blobs along the line of sight; the FWHM is only half an order of magnitude when the mean number of shells along a direction is 40 (fig. 1). The width of the distribution function is not sensitive to burst duration, and moreover it is almost independent of the energy fraction in magnetic field as long as ϵ_B is not so small that the shocks become almost adiabatic. It is also evident from fig. 1 that there are a number of bright spots in the cone containing the ejecta for which the observed isotropic γ -ray fluence is 5×10^{53} erg.

The fluence distribution function for the model consisting of collisions of uniform shells is similar to the graph in fig. 1. There are two differences, however, between the

uniform and the patchy shell models. One, the width of the fluence distribution function is smaller by a factor of ~ 10 for the uniform shell model with the same fixed total energy in explosion. The other difference is that the afterglow flux falls off smoothly in this model whereas in the case of inhomogeneous shells the afterglow flux at early time, within the first hour of the explosion, has large amplitude fluctuation. As discussed in §4 this can be used to observationally distinguish between the two models.

We have assumed that consecutive ejection of shells is completely random. It is possible that the energies of blobs ejected along a given line sight might have a non-zero correlation. It is straightforward to modify our calculation to include this correlation. We find that even for a perfect correlation of blob energy, and random distribution of Lorentz factor, the width of the distribution function for fluence is only slightly larger than the case where the correlation is zero (see §2.2 for discussion).

The integral probability distribution function is also shown in fig. 1. Note that the probability of seeing a burst with isotropic fluence of 7×10^{53} erg is about 0.1% (the total energy in explosion is fixed at 10^{52} erg). Thus, a particularly bright burst such as GRB990123, which was in the top 0.1% of all BATSE bursts, could well have had total energy in explosion similar to an average BATSE burst. In the case of GRB990123 we were perhaps looking at a very bright spot on the colliding shell surface.

This suggests that γ -ray fluence is not a reliable measure of the total energy in explosion. A more promising way to estimate the energetics of explosion is to consider emission at a later time when a number of causally disconnected regions have merged – but the shock is still radiative – thereby reducing the dispersion seen along different lines of sight. The ratio of the synchrotron cooling and the dynamical time is $t_s/t_d \approx 6\pi m_e c / (\sigma_T t_{obs} B^2 \gamma^2) \approx m_e / (\epsilon_B \sigma_T m_p c n_{ism} t_{obs} \gamma^4) \propto t_{obs}^{1/2}$, which becomes greater than 1 at $t_{obs} \sim 1$ hr. At this time $\gamma \sim 30$ and we expect about 20 disconnected regions to have merged, and the dispersion of the radiative flux along different lines of sights to have decreased by a factor of about 4. Note that the energy of the ejecta has also dropped by a factor of about 4 at this time.

2.2. Analysis of a simple model to understand the numerical results

We Analyze a simple model that captures some of the features of the numerical result presented above. Let us consider collision of two shells. The energy and the Lorentz factor of the outer (denoted by subscript 1) and the inner shell (subscript 2) are given by a distribution function $P_i(E, \gamma)$. The energy radiated when shells collide in some fraction of the total thermal energy produced in shell collision which is given by (cf. Kobayashi et al.

1998),

$$E_{col} = (E_1 + E_2) \left[1 - \left(\frac{E_1}{\gamma_1} + \frac{E_2}{\gamma_2} \right) \left(\frac{E_1^2}{\gamma_1^2} + \frac{E_2^2}{\gamma_2^2} + \frac{2E_1E_2\gamma_r}{\gamma_1\gamma_2} \right)^{-1/2} \right], \quad (1)$$

where $\gamma_r = \gamma_1\gamma_2(1 - v_1v_2) \approx \gamma_1\gamma_2(\gamma_1^{-2} + \gamma_2^{-2})/2$ is the relative Lorentz factor of collision of the shells. The thermal energy release is a function of $\gamma_2/\gamma_1 \equiv \eta$, and the energy radiated in some frequency band is a fraction of E_{col} . For instance, if electrons, magnetic field and protons are in equipartition, the energy radiated in 10–10³ keV is roughly $E_{col}/10$ (Kumar, 1999; Panaitescu et al. 1999). To simplify the analysis we calculate the bolometric fluence distribution function. The distribution in some other band is not all that different.

The bolometric distribution function is given by

$$P_{rad>(> F) = \int_{\gamma_{min}}^{\gamma_{max}} d\gamma_1 \int_{\gamma_1}^{\gamma_{max}} d\gamma_2 \int_{E_{1min}}^{\infty} dE_1 \int_{E_{2min}}^{\infty} dE_2 P_1(E_1, \gamma_1) P_2(E_2, \gamma_2), \quad (2)$$

where $E_{1min} \approx F/[(\eta + 1)(\eta^{1/2} - 1)^2]$ is the minimum energy of the outer shell, for a given $\eta = \gamma_2/\gamma_1$, so that the radiated energy is F , and $E_{2min} \approx 2F\eta^2/(\eta - 1)^2$ is the minimum energy of the inner shell to yield fluence F in shell collision.

Let us assume that the distribution functions are separable and write them as $P_i(E, \gamma) = P_{iE}(E)P_{i\gamma}(\gamma)$. Substituting this into equation (2) we obtain

$$P_{rad>(> F) = \int_{\gamma_{min}}^{\gamma_{max}} d\gamma_1 \int_{\gamma_1}^{\gamma_{max}} d\gamma_2 P_{1E}^c(E_{1min})P_{2E}^c(E_{2min})P_{1\gamma}(\gamma_1)P_{2\gamma}(\gamma_2), \quad (3)$$

where $P_{iE}^c(E) \equiv \int_E^{\infty} dE' P_{iE}(E')$.

Let us consider a particularly simple case where the distribution function for the inner and the outer shells are both constant in the intervals $(0, E_{max})$ and $(\gamma_{min}, \gamma_{max})$ and zero outside. The above equation can be easily integrated in this case and we find that the differential distribution function, $P'_{rad} \equiv dP_{rad}/dF$, is approximately proportional to $F^{-1/2}$ for $F \ll E_{max}/2 \approx F_{max}$, becomes steeper for $F \sim F_{max}$ and is zero for $F > F_{max}$. It can also be shown that for $P_{iE} \propto E^\alpha$, $P'_{rad}(F) \propto F^{-1/2}$ for $\alpha \geq 0$, and P'_{rad} falls off more steeply with F for $\alpha < 0$. For $P_{iE}(E) \propto \delta(E - E_0)$, $P'_{rad}(F) \propto F^{-1/2}$ as well i.e. the fluence distribution has a finite width even when the energies of all the blobs are identical.

Now we turn to collision of more than 2 shells. Let us assume that collision of any two shells gives rise to a distribution of fluence that is same as calculated above. This is a drastic simplification, nevertheless it provides useful insight into the qualitative behavior of the fluence-distribution function calculated in §2.2. The distribution function resulting from N collisions can be easily calculated and is given by:

$$P_{rad}^{(N)}(F) = \frac{1}{(2\pi)^{1/2}} \int_{-\infty}^{\infty} dk P'_{rad}(k) \exp(-ikF) \left[\int_0^F dF' P'_{rad}(F') \exp(ikF') \right]^{N-1}, \quad (4)$$

where $P'_{rad}(k)$ is the Fourier transform of $P'_{rad}(F)$. For $P'_{rad} \propto F^{-\alpha}$ we find from the above equation that $P_{rad}^{(N)}(F) \propto F^{(1+\alpha)N-1}$ for $F \ll F_{max}$, and it is zero for $F > NF_{max}$. The width of the distribution function on Log_{10} scale is $3/[(1-\alpha)N+2]$. The effective value of α is about 0.7 for the case where the energy spectrum of ejected shells is flat. The width calculated for the toy problem is somewhat smaller (for fixed N) than for the more realistic problem considered above because the energy produced in shell mergers decreases in successive mergers, hence the effective N for the merges is smaller than the number of shells expelled in the explosion. We show the distribution function for the model problem in fig. 2 for $\alpha = 0.5$ and 0.7.

To determine the effect of correlated ejection of shells we set $P_2(E_2, \gamma_2) = \delta(E_1 - E_2)P_{2\gamma}(\gamma_2)$ in equation (2). We find that for $F \ll F_{max}$, $P'_{rad}(F)$ is not very different from the case where shells were randomly ejected with no-correlation, whereas for $F \sim F_{max}$, the distribution function (P'_{rad}) falls-off somewhat more rapidly, which causes $P_{rad}^{(N)}$ to become a bit broader.

3. Comparison with observations

Table I depicts a compilation of the observations of GRBs and their afterglow with known redshifts. Included in the table is the observed isotropic γ -ray fluence (from Band et al., 1999), the X-ray luminosity after 5 hours (estimated from the published X-ray flux and the slope of the light curve), and the R-band magnitude 24 hours after the burst. To obtain a uniform sample we consider only bursts that have been observed by BATSE, for which there is a well determined fit for the spectrum using the Band function (Band et al., 1993). It can be seen from the table that while the spread in the isotropic γ -ray fluence is about two and a half orders of magnitude, the spread in the isotropic X-ray luminosity 5 hours after the burst, and the R-band optical luminosity at 1 day, is only about one and a half orders of magnitude.

These dispersions can be quantified. Consider first the six bursts with known redshifts and a well determined BATSE fluences². Assuming a normal distribution of $\log(E_\gamma)$ we find that the standard deviation of the logarithm of the (isotropic) energy emitted in

²Note that eight bursts appear in table I. However, the calculation of σ_γ is based on a

γ -rays, σ_γ , is 0.87. The corresponding FWHM is 2. The average isotropic γ -ray fluence is 1.4×10^{53} ergs. The likelihood is larger than 0.05 of the maximal value within the range $0.45 < \sigma_\gamma < 2.4$. Similar analysis for the isotropic X-ray luminosity 5 hours after the burst for six bursts yields: $\sigma_x = 0.58$, and FWHM of 1.4. The average (isotropic) X-ray luminosity is 1.3×10^{46} ergs/sec. A variance range for likelihood larger than 0.05 of the maximal likelihood is: $0.35 < \sigma_x < 1.45$. The standard deviation of the logarithm of the R-band luminosity 24 hours after the burst is $\sigma_R = 0.53$. We note that we have not corrected the observed flux for extinction and thereby have overestimated σ_R . A prediction of the patchy shell model is that σ_R should be smaller than σ_x . Current observations are consistent with this expectation, however more accurate determination of σ_R and larger number of afterglows are needed to improve the statistical significance of this result.

These results show that the FWHM of γ -ray energy distribution is wider by a factor of five than the X-ray afterglow luminosity distribution and is roughly consistent with the expected decrease in fluctuation amplitude by a factor of 7 based on the merger of causally disconnected regions (γ decreases by a factor of about 7 at 5 hr). If the γ -ray emitting surface were uniform (not highly patchy as considered here) and the large width of the isotropic γ -ray energy distribution were due to a wide distribution of the explosion energy (or the opening angle of the jet) then the distribution of afterglow luminosity in the X-ray and other wavelengths should have been wider than the γ -ray energy distribution since the afterglow flux $\log f_\nu = \frac{1}{4}(p+3) \log E + 0.5 \log n - \frac{3}{4}(p-1) \log t_{obs} + constant$; where $p \approx 2.5$, n is the density of the circumstellar medium, E is the energy in the explosion per unit solid angle so long as the opening angle of the ejecta is larger than $\gamma^{-1}(t_{obs})$, and the *constant* term includes the dependence on ϵ_e and ϵ_B . Assuming that E and n are uncorrelated, we expect the width of the afterglow luminosity, $\log(f_\nu)$, to be larger than the width of $\log E$ distribution by at least a factor of 1.4. Since the observed X-ray afterglow luminosity distribution is narrower by a factor of ~ 1.5 compared to γ -ray fluence (on log scale) this suggests that the distribution of E is very narrow³ and the large width of the γ -ray fluence distribution arises as a result of angular fluctuation in the γ -ray emitting surface.

subset of six bursts for which there is γ -ray data. Other subsets of six bursts are used to calculate σ_x and σ_R .

³The ratio of E and the observed isotropic γ -ray fluence is a constant of order 100, almost independent of E , in the internal shock scenario when shells are uniform.

4. Conclusions and Predictions

A relativistic shell ejected in an explosion could have large angular fluctuation because regions on the shell separated by an angle greater than γ^{-1} are causally disconnected. We have explored some consequences of the angular fluctuations in GRB explosions. Most of the results described here also apply to the model consisting of internal collisions of uniform shells.

We have modeled shells as consisting of independent blobs of angular size γ^{-1} . Because of relativistic beaming only a small patch of a shell, of angular size $\gamma^{-1} \sim$ the size of a blob, is visible to a distant observer.

The blobs are ejected in the explosion with some distribution of Lorentz factor and energy. We have calculated the spectrum of emergent photons which are produced by synchrotron plus inverse Compton processes in internal shocks when blobs undergo collisions, and find that the distribution of the observed γ -ray fluence along different lines of sights is very broad (the total energy in the explosion is fixed at 10^{52} erg). The width of the fluence distribution function depends on the width of the distribution of energy and the Lorentz factor of blobs; the FWHM of the $\log_{10}(\text{fluence})$ distribution function is 1.2 when the distribution of blob energy is a delta function, where as the width is 2 when the energy distribution of blobs, lognormal, has a FWHM of 1.

An intrinsic spread in the energy release in explosions, not considered here, will broaden the width of the observed γ -ray fluence distribution. The variation of the total explosion energy from one GRB to another will however give rise to fully correlated γ -ray and the afterglow emissions, which is at odds with observations.

In this scenario the emission surface of the expanding shells consists of bright patches, of angular width of order γ^{-1} , and dark patches; A bright GRB results not because of larger energy release in the explosion but instead when our line of sight intersects a bright spot on the expanding colliding shell, and thus the γ -ray fluence is not a good measure of the total energy release in the explosion.

The fluence distribution function resulting from collisions of uniform shells is similar in shape but smaller in width by factor of ~ 10 , for fixed total energy in explosion, compared to when shells have large angular fluctuations. For the sub-class of GRBs which show short timescale variability, the observed γ -ray fluence for the uniform shell model is proportional to the energy in explosion, and the width of the distribution function in this case is equal to the width of the total energy release in explosions.

The $\sim 1\%$ radiative efficiency of internal shocks (Kumar, 1999; Panaitescu, Spada and Mészáros 1999) in $10\text{--}10^3$ keV energy band requires total energy in explosion to be larger than the observed energy in γ -ray photons by a factor of about 100. The finite opening

angle for burst ejecta reduces the energy requirement by a factor of 10–100. The angular inhomogeneity of shells ejected in the explosion could further reduce the energy budget of the brightest bursts, such as GRB990123, by a factor of ~ 10 thereby bringing down the total energy involved in the brightest observed bursts to a value of order the energy in weaker bursts i.e. $\lesssim 10^{53}$ erg.

An interesting result of this model is that in spite of the very wide observed luminosity function of GRB, the total energy in GRB explosions could be roughly comparable in all bursts. This could have interesting implications on the nature of the inner engine.

There are several predictions of our model. First, the width of the distribution function in the X-ray afterglow flux should be significantly smaller than the spread of fluence seen in γ -rays. Moreover, the dispersion of optical luminosity should be smaller than the X-ray luminosity, and the late time radio afterglow should have the smallest dispersion which reflects the variation of energy in GRB explosions. The γ -ray, X-ray, and the optical data for GRBs with known redshifts are consistent with these expectations.

It should be noted that the observed decrease in the width of the isotropic luminosity distribution for the afterglow emissions, compared to the width of the isotropic γ -ray fluence distribution, is contrary to what is expected if the width of the fluence distribution were a consequence of a wide distribution of energy release in GRBs (see §3).

A second prediction is that the afterglow flux should show small amplitude fluctuation with time if the energy distribution of blobs is not a delta function or shells are not uniform. For instance, the fluctuation amplitude 1 day after the explosion, when the FWHM of blob energy distribution is 10, is ~ 0.02 mag in the optical band and the characteristic variability timescale is ~ 1 day. The early afterglow light curve should show however larger fluctuations whose amplitude decreases in time. This prediction could be directly tested with the forthcoming quick response GRB missions, HETE II, Swift and BALERINA, and thereby distinguish between the uniform and fluctuating shell models.

A third prediction is the existence of numerous weak bursts - which will arise from the low energy tail of the GRB luminosity function. The afterglow flux from these weak bursts should be comparable to the afterglow from stronger bursts - this may have implications to the rate of “orphan” afterglows.

A fourth prediction is that the fluence distribution of multi peaked bursts (which arise due to numerous collisions) would be narrower than the fluence distribution of bursts with only a few peaks. Most of the bursts detected by BeppoSAX, for which afterglow emission and redshifts have been measured, show light curves consisting of a few peaks which could arise as a result of collision of just a few shells. For such bursts we expect very wide fluence distribution as observed.

Finally, as the prompt optical and the prompt X-ray emissions arise in regions which

are moving with very high Lorentz factor (Sari and Piran, 1999) we expect these emissions to also have a very wide luminosity function, whose width should be comparable to the GRB luminosity function i.e. the prompt emission could be dominated by small hot spots and produce unusually large fluences in some cases. As mentioned earlier we expect temporal fluctuations with a decreasing amplitude in time during this stage.

We thank Reem Sari for helpful remarks. This research was supported by the US-Israel BSF 95-328, by a grant from the Israeli Space Agency and by a NASA grant NAG5-3091. TP thanks F.-K. Thielemann and the Physics department of Basel University for hospitality while this research was done. PK thanks Savannah for encouraging him to investigate the fireball model.

REFERENCES

- Band, D., et al. 1993, ApJ 413, 281
- Band, D., Jimenez, R. & Piran, T., 1999, in preparation
- Bond, H.E. 1997, IAU Circ. 6654
- Costa, E., et al. 1997, IAU Circ. 6572
- Frail, D.A. et al. 1997, Nature 389, 261
- Harrison et al. 1999, astro-ph/9905306
- Kobayashi, S., Piran, T. & Sari, R. 1997, ApJ 490, 92
- Kulkarni et al. 1999, Nature 398, 389
- Kumar, P., 1999, to appear in ApJ letter
- Mészáros, P., & Rees, M.J. 1997, ApJ 476, 232
- Narayan, R., Paczynski, B. & Piran, T. 1992, ApJ 395, L83
- Paczynski, B. & Xu, G. 1994, ApJ 427, 708
- Panaitescu, A., Spada, M. & Mészáros, P., 1999, astro-ph/9905026
- Piran, T. 1999, Physics Reports, 314, 575.
- Sari, R., & Piran, T. 1997a, MNRAS 287, 110
- Sari, R., & Piran, T. 1997b, ApJ 485, 270
- Sari, R., & Piran, T. 1999, ApJ, 520, 641
- Sari, R., & Piran, T. & Halpern, J. 1999, ApJ 519, L17
- Sari, R., & Piran, T. & Narayan, R. 1998, ApJ 497, L17
- van Paradijs, J., et. al. 1997, Nature 386, 686

GRB	Z	F_γ ¹	F_γ ²	E_{iso}	$F_x(5hr)$ ³	$L_x(5hr)$ ⁴	R(24hr)	$L_{opt}(24hr)$ ⁵
		$10^{-5} \frac{\text{ergs}}{\text{cm}^2}$	$10^{-5} \frac{\text{ergs}}{\text{cm}^2}$	10^{53} ergs	$10^{-12} \frac{\text{ergs}}{\text{cm}^2 \text{sec}}$	$10^{46} \frac{\text{ergs}}{\text{sec}}$		$10^{44} \frac{\text{ergs}}{\text{sec}}$
990510	1.619	2.26	2.94	1.5	-	-	19.5	2.8
990123	1.6	26.8	34.9	18	13.5	8.9	20.5	1.1
980703	.967	2.26	3.0	0.54	5.9	1.6	20.7	0.37
980613	1.096	-	-	-	0.82	2.7	22.9	0.06
971214	3.412	0.944	1.11	3.2	1.97	4.2	22.5	0.54
970828	0.958	9.60	13.9	3.0	5.57	1.5	-	-
970508	0.835	0.317	0.55	0.054	1.10	0.22	21.2	0.18
970228	0.695	-	-	-	-	-	21.2	0.13

Table 1: A comparison of the afterglow and the γ -ray luminosities for GRBs with known redshift. The total isotropic energy in γ -rays, the X-ray luminosity after 5 hours in 2–10 keV, and the optical luminosity in the R band after 1 day are calculated assuming a flat Universe with $\Omega_\Lambda = 0.7$ and $h = 60$.

1. The observed fluence in 10keV–2MeV range (from Band et al. 1999).
2. The γ -ray fluence after K correction based on a detailed fit of the spectrum (from Band et al. 1999).
3. X-ray flux, 5 hr after the burst, in 2–10 keV energy band.
4. X-ray luminosity in 2–10 keV using a K correction corresponding to a spectrum $\propto \nu^{-0.75}$.
5. Using a K correction corresponding to a spectrum $\propto \nu^{-0.75}$. Note that there is no extinction correction.

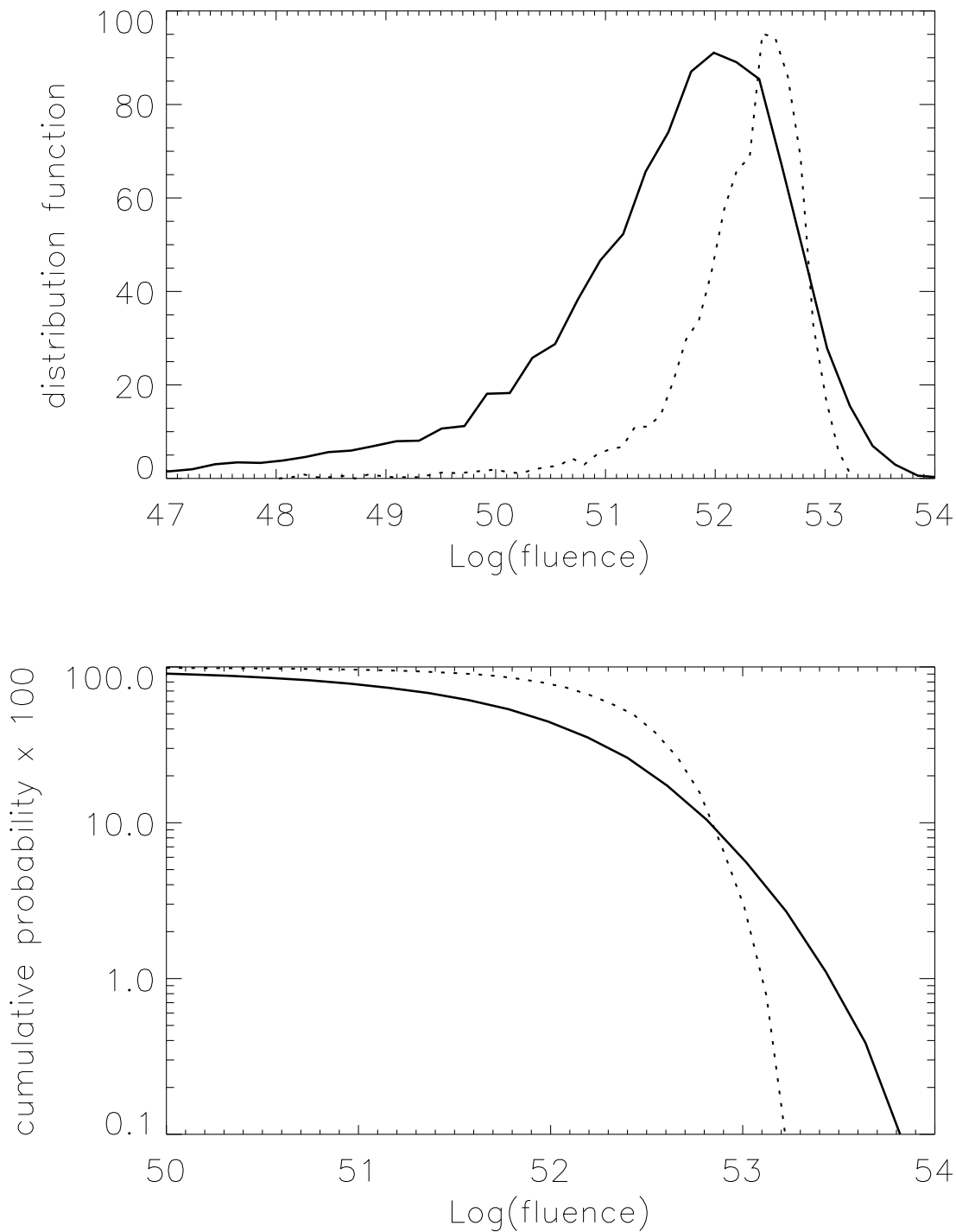


Fig. 1.— The distribution of GRB fluence in $10\text{--}10^3$ keV band (top panel). The mean number of shells ejected along a fixed direction is 5 for solid curve and 40 for the dotted curve. The energy in the explosion, where material is ejected in a cone of opening angle 10° , is taken to be 10^{52} erg. Moreover, the burst duration is 30 s, and $\gamma_{min} = 5$ & $\gamma_{max} = 400$.

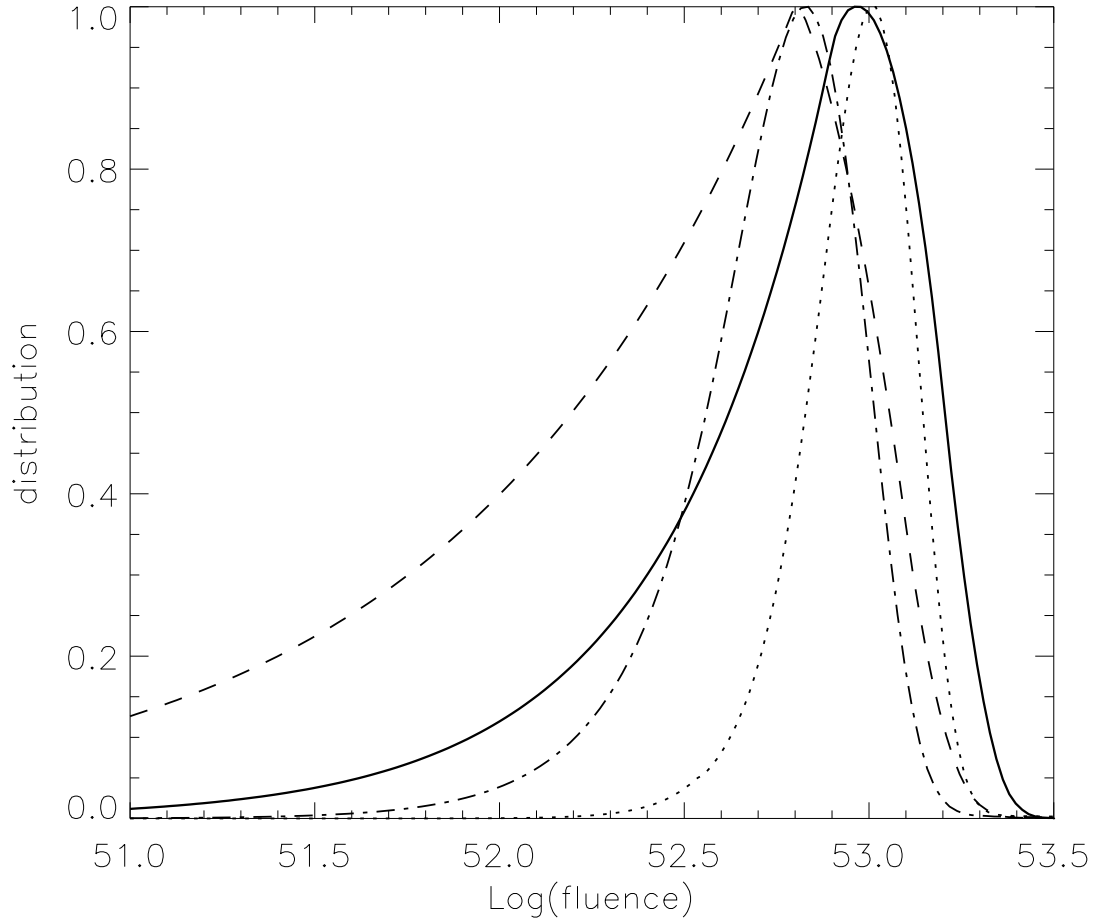


Fig. 2.— The probability distribution function for the toy model discussed in §2.3. The four different curves are for different values of (α, N) — $(0.5, 4)$ for the solid curve, $(0.5, 10)$ for the dotted curve, and for the dashed and dash-dot curves the values are $(0.7, 5)$ and $(0.7, 10)$ respectively.